

# Synthesis and Characterization of Electropolymerized Poly(2-amino-3-cyano-4- $\beta$ -naphthylthiophene)

Duygu Ekinçi, Ferhan Tümer, and Ümit Demir\*

Department of Chemistry, Atatürk University, Arts and Sciences Faculty, 25240 Erzurum, Turkey

Received January 13, 2004; Revised Manuscript Received June 11, 2004

**ABSTRACT:** Novel aminothiophene-based dimer, oligomers, and polymer were synthesized by the electrochemical oxidation of 2-amino-3-cyano-4- $\beta$ -naphthylthiophene ( $\beta$ -ACNT). These products obtained after a preparative electrolysis were characterized by FTIR,  $^1\text{H}$  and  $^{13}\text{C}$  NMR, FAB-MS, and UV–vis–NIR spectroscopy. Additionally, scanning tunneling microscopy (STM) was used to investigate the thin film morphology of polyaminothiophene. Results showed that 2-amino-3-cyano-4- $\beta$ -naphthylthiophene could be electropolymerized, leading to one stable dimer, which has a long conjugation length with a fluorescent property at 538 nm, and a mixture of oligoaminothiophenes. UV–vis–NIR spectroelectrochemistry of a thin film of polyaminothiophene on ITO shows low-energy absorptions at 542, 830, and 1050 nm, which are blue-shifted compared to the absorptions obtained in solution. STM results indicate that the surface of single crystalline Au(111) is completely covered with a highly oriented thin film of polymer.

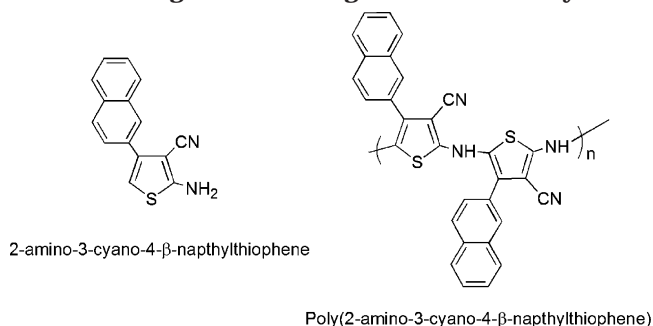
## 1. Introduction

Conjugated oligomers and polymers derived from thiophene and its derivatives have recently emerged as very promising materials for electronics and optoelectronics such as electrochemical capacitors,<sup>1</sup> cathode materials for battery,<sup>2</sup> and electrochromic displays.<sup>3,4</sup> The interest in the synthesis of novel materials with new properties has increased considerably during the past decade. One of the strategies to synthesize novel materials is to modify the monomer structure by introducing different substituents to a monomer skeleton.<sup>5,6</sup> Since the electrical, optical, and mechanical properties of polymers depend strongly on the structure and the stereoregularity of the monomeric starting material,<sup>7</sup> an alternative strategy is to design a new monomer, which has the activated position to increase the selectivity in the coupling during polymerization.<sup>8</sup>

Inspired by the challenge of designing low-band-gap polymers with intense NIR absorption, we focused our attention on a novel class of conjugated oligomers derived from aminothiophene electrochemically, which has an amino group attached to the 2-position in order to activate this position. Although the electrochemical polymerization of aniline and thiophene derivatives has been extensively investigated, there is no study about the electrochemical behavior of aminothiophene and its derivatives in the literature so far. In the preceding papers,<sup>9,10</sup> we have reported that the electrooxidation mechanisms of 2-amino-3-cyano-4-phenylthiophene (ACPT) was similar to those common aromatic amino compounds. Furthermore, we have found out that ACPT could be electropolymerized leading to a mixture of oligoaminothiophenes, which has long conjugation length with a fluorescent property at 520 nm.

We report here the synthesis and characterization of a new class of polymer derived from 2-amino-3-cyano-4- $\beta$ -naphthylthiophene ( $\beta$ -ACNT), formed by introducing the naphthyl group at the 4-position of aminothiophene in order to get longer conjugation length (Scheme 1).

**Scheme 1. Structure of Aminothiophene Monomer and Oligomers Investigated in This Study**



The aminothiophene system is of interest not only in synthesis of a new class of conducting polymers but also for understanding of the electrooxidation mechanisms of aminothiophenes which bear a resemblance to the properties of aniline and thiophene. The characterization of the resulting polymer films were carried out by several techniques [cyclic voltammetry, UV–vis–NIR, Fourier transform infrared (FTIR),  $^{13}\text{C}$  and  $^1\text{H}$  NMR, and FAB mass spectroscopy]. The morphology of thin film of polymer was also analyzed by scanning tunneling microscopy (STM).

## 2. Experimental Section

**2.1. Synthesis and Characterization of  $\beta$ -ACNT.** 2-Amino-3-cyano-4- $\beta$ -naphthylthiophene has been prepared following a previously reported procedure.<sup>11</sup> The product was purified via column chromatography (neutral  $\text{Al}_2\text{O}_3$ ) with chloroform–hexane as eluents. FAB+ mass spectrum:  $m/z$  250 ( $\text{M}^+$ , 100%), 251 ( $\text{MH}^+$ , 75%). FTIR (KBr): 3428, 3326, 3122, 3054, 2204, 1640, 1619, 1514, 1402, 1198  $\text{cm}^{-1}$ .  $^1\text{H}$  NMR (200 MHz,  $\text{CDCl}_3$ , ppm):  $\delta$  = 8.09 (1H, s, ArH), 7.92–7.48 (6H, m, Ar–H), 6.47 (1H, s, H5), 4.94 (2H, bs,  $\text{NH}_2$ ).  $^{13}\text{C}$  NMR (50 MHz,  $\text{CDCl}_3$ , ppm):  $\delta$  = 165.55, 141.98, 135.39, 134.99, 133.52, 130.52, 130.31, 129.67, 128.49, 128.38, 128.09, 127.15, 117.83, 108.38, 90.84.

**2.2. Chemicals and Reagents.** Acetonitrile (Fluka Chemical) “MeCN” was purified by drying with calcium hydride, followed by distillation from phosphorus pentoxide. After purification in order to eliminate its water content as much

\* To whom correspondence should be addressed: Tel +90-442-2314434; Fax +90-442-236 0948; e-mail udemir@atauni.edu.tr.

as possible, it was kept under molecular sieves (3A, Merck). Tetrabutylammonium perchlorate, TBAClO<sub>4</sub> (Fluka Chemika), and all other chemicals were of reagent grade and were used as received.

**2.3. Electrochemistry.** Electrochemical studies were carried out with a BAS 100B/W electrochemical workstation equipped with a low-current module (BAS PA-1) at a platinum disk electrode. Cyclic voltammetric measurements were made at room temperature in an undivided cell (BAS model C-3 cell stand) with a platinum counter electrode and an Ag/Ag<sup>+</sup> reference electrode (BAS). All potentials are reported with respect to Ag/Ag<sup>+</sup>. The solutions were deoxygenated by passing dry nitrogen through the solution for 30 min prior to the experiments, and during the experiments the flow was maintained over the solution. The platinum disk electrode was mechanically polished with an alumina paste (10  $\mu$ m) to the mirror finish and then rinsed with distilled water and acetonitrile for several times. ITO-coated glass electrodes (Delta Technologies) were cleaned by sonication in a detergent solution for 5 min and then rinsed with a large amount of doubly distilled water. Further sonication in ethanol for 5 min was done before being blown dry with a stream of nitrogen.

**2.4. Spectroscopy.** <sup>1</sup>H NMR (200 MHz) and <sup>13</sup>C NMR (50 MHz) spectra were recorded with a Varian-Gemini 2000 spectrometer. FTIR spectra (KBr) were run on a Mattson 1000 FTIR spectrometer. FAB mass spectra were obtained with a JEOL JMS-HX 110A double-focusing mass spectrometer equipped with an XMS data system. A fast-atom xenon beam was generated from Xe<sup>+</sup> ions, which were accelerated to 1 kV with a FAB gun emission current of 1 mA. The samples were placed on the stainless steel tip of the probe, mixed with *m*-nitrobenzyl alcohol (Aldrich) as a matrix, and exposed to the xenon beam for the desorption. Absorption and emission measurements were obtained using the double-beam Shimadzu UV-vis-NIR 3101 PC scanning spectrophotometer and a Shimadzu RS 5301 spectrofluorophotometer.

Spectroelectrochemistry experiments were carried out in an absorption cuvette modified as an electrochemical cell. A platinum working electrode, a platinum counter electrode, and a reference electrode are placed into this cell so that electrodes are away from the path of the light. The electronic spectra of thin film were recorded by placing the ITO electrode in the path of the sample light beam.

STM data were acquired in air using a Molecular Imaging Model PicoScan instrument. In all cases, Pt-Ir tips were used for imaging. Experimental conditions are given in the figure captions; positive bias voltages indicate that the tip was positive relative to the sample.

### 3. Results and Discussion

**3.1. Electrooxidation of 2-Amino-3-cyano-4- $\beta$ -naphthylthiophene.** The anodic oxidation of  $\beta$ -ACNT was performed in anhydrous acetonitrile solutions containing 0.5 M TBAClO<sub>4</sub> at a platinum disk electrode. The cyclic voltammogram of 5.0 mM  $\beta$ -ACNT shows an irreversible oxidation peak (I) at the potential of 1190 mV at the first scan (Figure 1). Reversing the potential, two well-defined reductive peaks are observed at potentials of 810 mV (II) and 470 mV (III) shown in Figure 1. In the second and subsequent positive sweeps, two new oxidation peaks appear at 715 mV (IV) and 870 mV (V), indicating that new electroactive species were formed after the first anodic peak.

These results show, in agreement with those of diphenylamine, aniline, and 4-aminobiphenyl voltammograms, that the anodic oxidation of  $\beta$ -ACNT may follow an E(CE)<sub>*n*</sub>-type mechanism and that the products are more easily oxidized than the parent compound.<sup>12–16</sup> Even though, the kinetic parameters estimated by combining cyclic voltammetric experiments and digital simulations for the best fittings indicates that the dominant step of the dimerization of  $\beta$ -ACNT is the

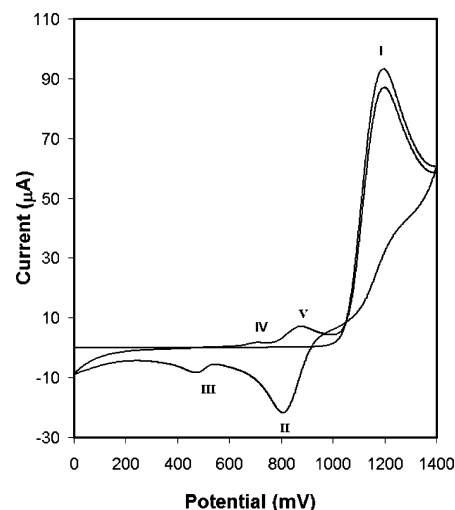


**Figure 1.** Cyclic voltammogram of 5.0 mM  $\beta$ -ACNT in dry MeCN solution containing 0.1 M TBAClO<sub>4</sub>; sweeps between 0.0 and 1.4 V. Scan rate: 100 mV s<sup>-1</sup>. Working electrode platinum disk.

radical cation–radical cation coupling, which leads to stable dimers.<sup>17</sup> We found that the coupling of dimeric cation radical of CR-PM with neutral  $\beta$ -ACNT molecules or the other radicalic species is the main pathway for the oligomerization and polymerization.

**3.2. Bulk Electrolysis of  $\beta$ -ACNT.** Potential-controlled bulk electrolysis of  $\beta$ -ACNT was carried out at the potential of 1210 mV, which is 20 mV more positive than the peak potential of peak I (Figure 1). An initially colorless monomer solution turns to green first then to a reddish-brown. During the electrolysis the height of the peak I decreased but not disappeared completely. However, at the end of the electrolysis half of starting monomer has been recovered. The electrolysis products (dimer, oligomeric mixture, and polymer) were separated by column chromatography. The products were characterized with FAB+ MS, <sup>1</sup>H and <sup>13</sup>C NMR, FTIR, and UV-vis-NIR spectroscopic techniques.

**3.3. Characterization of Dimer.** The cyclic voltammogram taken after exhausted electrolysis showed the peak II/V did not disappear due to the formation of stable dimer, whereas the peak III/IV disappeared completely at the end of electrolysis, resulting in oligomers and finally polymer. Therefore, we intended to isolate the stable dimer formed at the potential of peak V and characterize it.

Figure 2 shows the cyclic voltammogram obtained from second eluent from column chromatography. As can be seen, the cyclic voltammogram from the second eluent has a similar voltammetric behavior compared with the peak II/IV in Figure 1 but shifted to less positive potentials.  $\Delta E_p$  ( $E_{p,V} - E_{p,II}$ ) in Figure 1 is larger in potential than  $\Delta E_p$  for the peaks II/V in Figure 2 due to electrode is partially covered by the polymers, and there are interaction forces between the dimer and the other species in the solution such as monomer and oligomers, which causes the potential shift and larger  $\Delta E_p$ . The redox wave has a reversible electrochemical behavior at all scan rates in MeCN + 0.1 M TBAClO<sub>4</sub> solutions, indicating that the corresponding product is very stable in the absence of monomer or other radicalic species. Figure 3a presents the positive FAB mass spectra of the second eluent, with a molecular ion at *m/z* 498, the base peak, corresponds to the dimer formed because of electrochemical oxidation of  $\beta$ -ACNT.

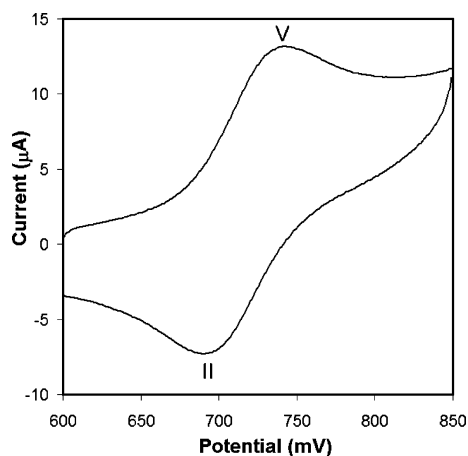


**Figure 2.** Cyclic voltammogram of isolated D1 dimer in anhydrous MeCN solution containing 0.1 M TBAClO<sub>4</sub>. Scan rate: 100 mV s<sup>-1</sup>.

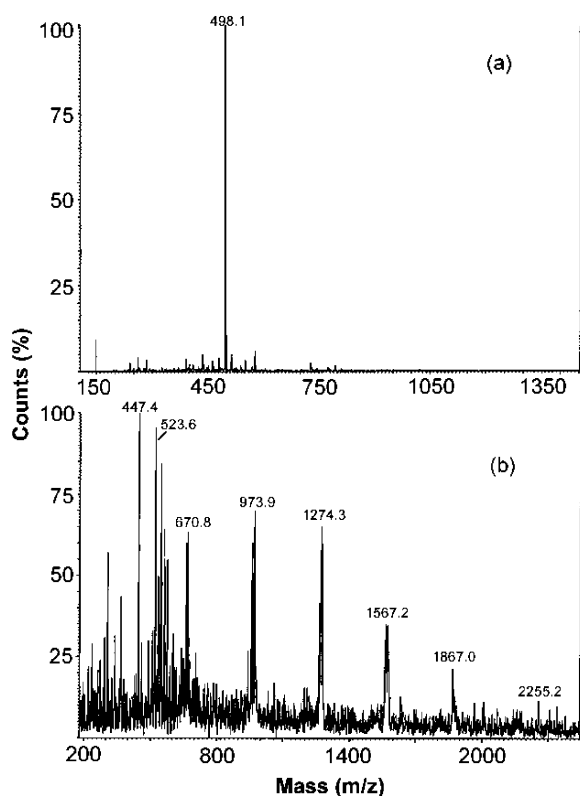
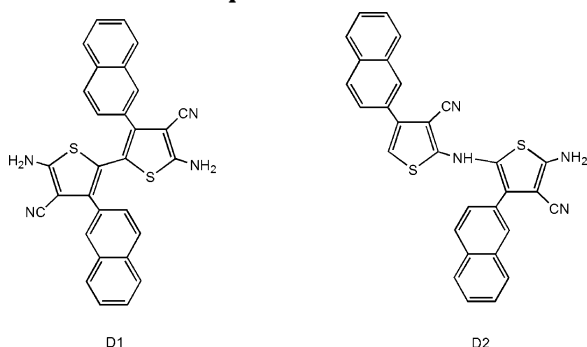


**Figure 3.** FAB mass spectra of (a) dimer and (b) oligomeric mixture.

#### Scheme 2. Proposed Structure of Dimers



Since both D1 and D2 dimers (Scheme 2) have the same molecular weight, additional spectroscopic methods have been employed for characterization of this

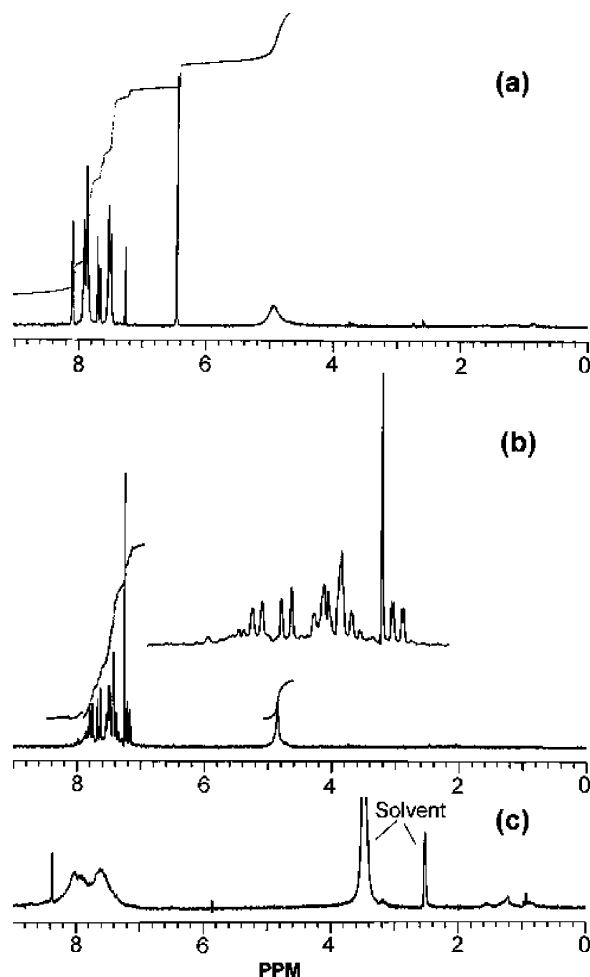


**Figure 4.** <sup>1</sup>H NMR spectrum of (a) β-ACNT in CDCl<sub>3</sub>, (b) dimer in CDCl<sub>3</sub>, and (c) oligomeric mixture in CD<sub>3</sub>OD.

dimer. The typical <sup>1</sup>H NMR spectra of monomer and dimer are given in Figure 4a,b. Although the multiplet resonance between 7.4 and 8.1 ppm and the broad resonance at 4.94 ppm appear in two spectra, the singlet resonance at 6.4 ppm for the proton attached to C5 (H5) in the monomer spectrum is absent in the dimer spectra. This observation indicates that the coupling occurs between C5 carbons in the thiophene ring. This conclusion is supported by <sup>13</sup>C NMR spectra. The resonance of tertiary carbon at 108 ppm in monomer (Figure 5.a) disappeared after the coupling, and a new signal appeared at 116 ppm due to quaternary carbon because of formation of C–C bond (Figure 5b). All these spectroscopic results indicate that the corresponding stable dimer is D1 (Scheme 2).

**3.4. Characterization of Oligomer.** Figure 3b shows the FAB mass spectra obtained from the soluble part of the reaction mixture. No attempt has been made to assign each of the individual peaks in the spectra due to the fragmentation process of oligomers with high molecular weight, which occur in the FAB-MS source.<sup>18</sup> As shown in the spectra, the molecular weight distribution of fragments is concentrated at *m/z* 670.8, 973.9, 1274.3, 1567.2, and 1867.0, matching to different chain length of oligomers. The largest fragment peak appeared at *m/z* 2255.2, which approximately corresponds to nine units of the monomer.

The <sup>1</sup>H NMR of the oligomeric mixture in Figure 4c consists of a series of resonances superimposed on two rather broad absorptions centered at 7.6 and 8.0 ppm.

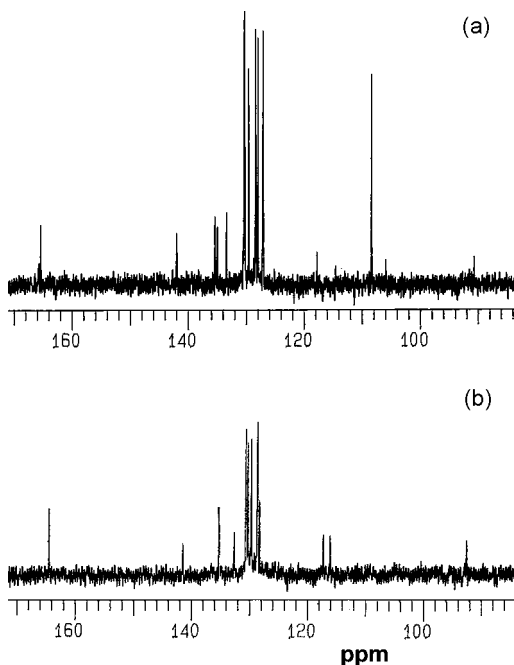


**Figure 5.**  $^{13}\text{C}$  NMR spectrum of (a)  $\beta$ -ACNT in  $\text{CDCl}_3$  and (b) dimer in  $\text{CDCl}_3$ .

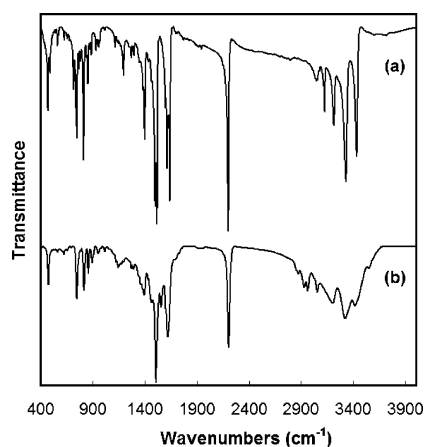


**Figure 6.** FTIR spectra of (a)  $\beta$ -ACNT and (b) oligomeric mixture of  $\beta$ -ACNT.

The broad features in the spectrum appear to be a manifestation of a number of closely spaced and overlapping individual proton resonances. This is to be expected since there are too many similar proton resonances in the polymeric material, which appears to contain a range of oligomers. The sharp resonance observed at 8.2 ppm is attributed to the NH protons, which are tended to shift when different solvent is used to take spectra.

This observation was also confirmed by FTIR (Figure 6). For the monomer spectrum, bands at 3429, 3301, and 3209  $\text{cm}^{-1}$  are assigned as N–H stretching modes.<sup>10</sup> The band ascribed as the NH stretching for the primary amino groups at 3429  $\text{cm}^{-1}$  in monomer spectra almost disappeared at the spectra for the oligomeric mixture, indicating that coupling occurs between carbon at the 5-position in the thiophene ring and nitrogen of the amino group in the polymerization processes. Another significant difference is that a new strong band at 1602  $\text{cm}^{-1}$ , attributed to the C=N stretch of the imino groups,<sup>19,20</sup> appears while the band at 1627  $\text{cm}^{-1}$  (C–NH<sub>2</sub>) gets weaker in intensity. These FTIR results

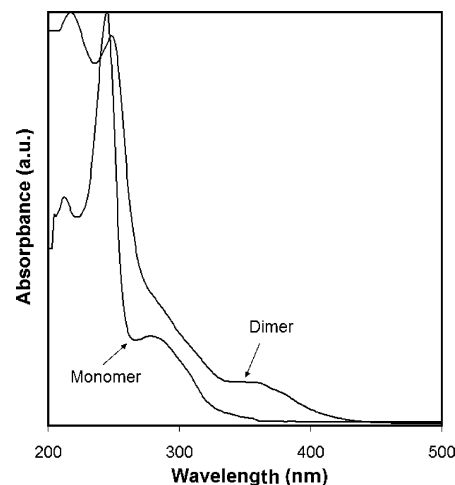


**Figure 7.** UV-vis-NIR spectrum of  $\beta$ -ACNT monomer and dimer in MeCN.

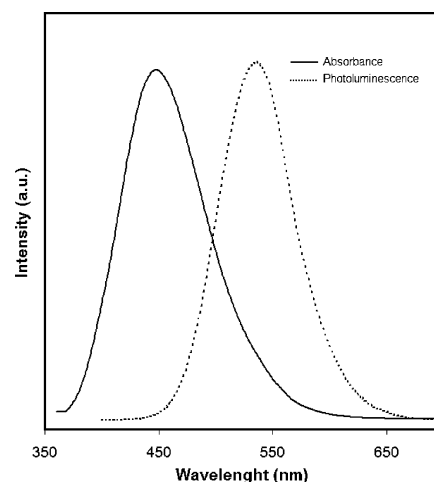


**Figure 8.** Photoluminescence spectra of dimer in MeCN.

suggest that the  $-\text{NH}_2$  group takes part in the electropolymerization and agree with that expected for the mixture of quinoidal and benzenoid form of oligoaminothiophene. A similar observation has been shown for the mixture of reduced and oxidized form of polyaniline and related oligomers.<sup>21,22</sup> The existence of a band at 2210  $\text{cm}^{-1}$  characteristic of a nitrile group and the absence of SH and C=O group in the FTIR spectrum is a sign of conversion of the monomer structure in oligomeric structure.

**3.5. UV-vis-NIR Spectroscopy.** The UV-vis-NIR spectra of monomer, dimer (D1), and oligomeric mixture in acetonitrile are shown in Figure 7 for comparison. The typical absorption peaks at  $\lambda_{\text{max}} = 214$  and 279 nm due to the  $\pi \rightarrow \pi^*$  transition in the monomer decreases in intensity, and a new broad absorption band at 370 nm appears in the dimer spectra. This band corresponds to the  $\pi-\pi^*$  transition whose energy depends on the  $\pi$ -electron delocalization, indicating that resulting dimer have more extended  $\pi$ -systems than monomer. As expected, the maximum of absorption in the UV-vis-NIR range or oligomeric mixture goes to longer wavelengths (515, 796, and 1030 nm) as the conjugation length (the consecutive thiophene units) increases. The shift for the  $\lambda_{\text{max}}$  is in agreement with the previous study for the dicyanooligothiophenes with 5–6 monomer units obtained by Barclay.<sup>23</sup>



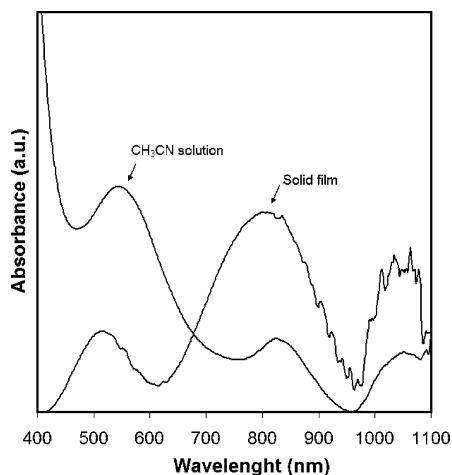


**Figure 9.** UV-vis-NIR spectra of poly( $\beta$ -ACNT) in MeCN and polymeric film on ITO electrode.

The overlaid absorption and emission spectra for the dimer (D1) are presented in Figure 8. The excitation of dimer by a 432 nm wavelength radiation in DMSO gives photoluminescence at about 538 nm, which can be seen with the naked eye. Similar photoluminescence was also observed for oligomeric mixture in both solution and solid state. It is evident from the UV-vis-NIR and emission spectra that product have much higher degree of conjugation than the corresponding monomer.

### 3.6. Characterization of Polymeric Thin Films.

To examine the absorption of thin film of polyaminothiophene, we carried out in situ spectroelectrochemistry on transparent indium tin oxide (ITO) electrodes. The cyclic voltammograms of electrooxidation of  $\beta$ -ACNT were similar to those obtained on Pt electrodes, although the position of all peaks were slightly shifted due to the resistance of the ITO layer. A thin film of poly( $\beta$ -ACNT) was deposited on ITO electrodes by cycling the potential between 400 and 1200 mV for 10 times. The spectroelectrochemical studies of the films exhibited the same spectrum with the solution spectra in the UV-vis-NIR range (Figure 9). However,  $\lambda_{\text{max}}$  of the absorption peaks of the thin film of polymer deposited on ITO are at higher energy than the one obtained in solution. Normally, we expect a red shift due to the more ordered conformation and an increase in  $\pi$ -conjugation length in condensed state. A similar blue shift has been observed for the other conjugated polythiophene systems due to the more coplanar and robust configuration of the quinoid structure of the polymer which leads to less freedom of the interannular rings.<sup>24,25</sup> Theoretical considerations have shown that band gap (Eg) should decrease as a function of the increase in the quinoid character of the  $\pi$ -conjugated system at the expense of its aromaticity.<sup>26</sup>

The film morphology was analyzed by scanning tunneling microscopy by using the Au (111) single crystalline electrode as a substrate, and the images of Au(111) before and after the deposition of thin films of poly( $\beta$ -ACNT) are presented in Figure 10a,b. Since this substrate consists of atomically flat surfaces, we can use this flat surface as a reference surface. The STM images obtained after electrochemical deposition show that the electrode surface completely covered with thin films of poly( $\beta$ -ACNT). On the other hand, the film consists of long grains with 200 nm width oriented horizontally to each other. This observation indicates that the strong intermolecular  $\pi$ -stacking forces causes to preferential

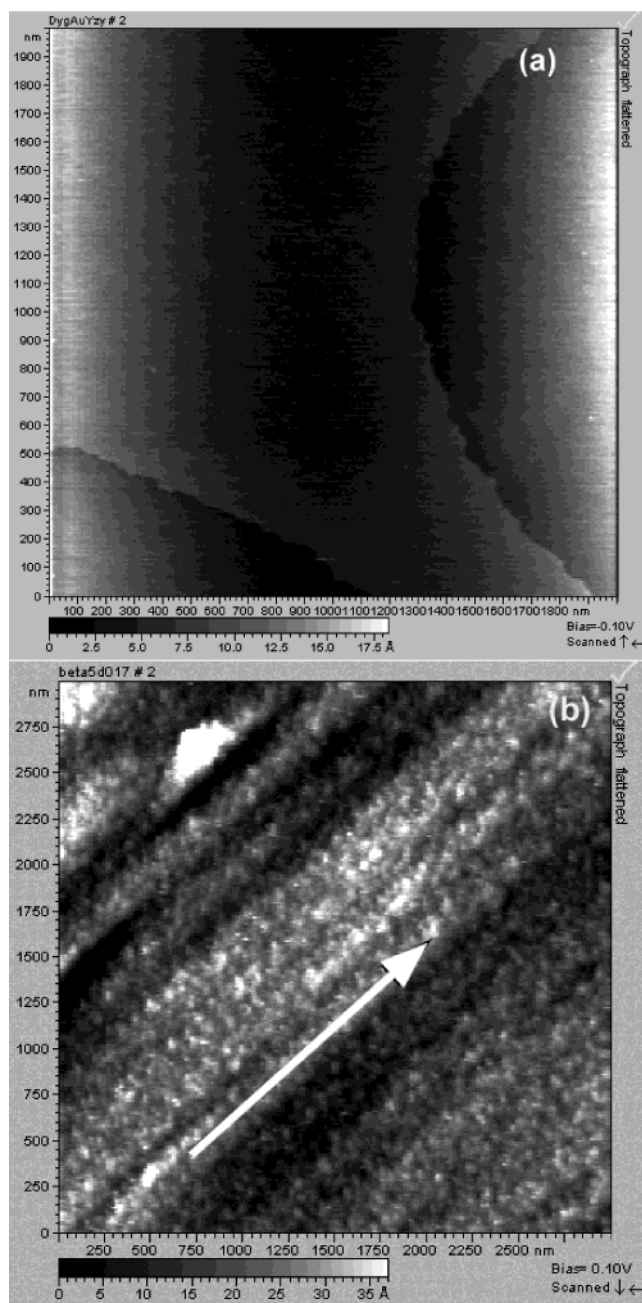


**Figure 10.** Scanning tunneling microscopy images of bare (a) and thin film of poly( $\beta$ -ACNT) deposited Au(111) single crystalline substrate (b).

orientation of the oligomers or polymer chains in the film.

## 4. Conclusions

We have shown here for the first time that 2-amino-3-cyano-4- $\beta$ -naphthylthiophene could be electropolymerized leading to a stable dimer, which is very stable and can be isolated and characterized spectroscopically as a minor intermediate product after preparative electrolysis, a mixture of oligaminothiophenes and polymer. UV-vis-NIR spectroscopic studies revealed that the polymer and oligomeric mixture in both solution and solid state have the same low-energy absorptions. However, the absorption maxima for thin film of polymer prepared by the electrochemical deposition on ITO electrodes were blue-shifted due to quinoid structure of the polymer. STM images of polyaminothiophene thin

films formed on single crystalline Au(111) show them to be compact and of a regular structure. Further investigations toward the synthesis of new polyaminothiophenes by modification of monomer and the isolation and characterization of this oligoaminothiophene mixture are in progress, which may result in a new class of materials with luminescent property.

**Acknowledgment.** The Scientific and Technical Research Council of Turkey (TUBITAK, TBAG-1984 (100T093)) and Atatürk University are gratefully acknowledged for the financial support of this work.

## References and Notes

- (1) Roncali, J. *Chem. Rev.* **1997**, *97*, 173–205.
- (2) Jelle, B. P.; Hagen, G.; Nodland, S. *Electrochim. Acta* **1993**, *38*, 1497–1500.
- (3) Gustofsson, J. C.; Inganas, O.; Andersson, A. M. *Synth. Met.* **1994**, *62*, 17–21.
- (4) Grunathan, K.; Murugan, A. V.; Marimuthu, R.; Mulik, U. P.; Amalnerkar, D. P. *Mater. Chem. Phys.* **1999**, *61*, 173–191.
- (5) Ng, M. K.; Wang, L.; Yu, L. *Chem. Mater.* **2000**, *12*, 2988–2995.
- (6) Greve, D. R.; Apperloo, J. J.; Janssen, R. A. *Eur. J. Org. Chem.* **2001**, *18*, 3437–3443.
- (7) Loeve, R.; McCullough, R. D. *Chem. Mater.* **2000**, *12*, 3214–3221.
- (8) Welzel, H. P.; Kossmehl, G.; Stein, H. J.; Schneider, J.; Plieth, W. P. *Electrochim. Acta* **1995**, *40*, 577–584.
- (9) Ekinci, D.; Horasan, N.; Altundaş, R.; Demir, Ü. *J. Electroanal. Chem.* **2000**, *484*, 101–106.
- (10) Ekinci, D.; Tümer, F.; Demir, Ü. *Eur. Polym. J.* **2002**, *38*, 1837–1843.
- (11) Gewald, K. *Chem. Ber.* **1965**, *98*, 3571–77.
- (12) Yang, H.; Bard, A. J. *J. Electroanal. Chem.* **1991**, *306*, 87–109.
- (13) Guay, J.; Dao, L. H. *J. Electroanal. Chem.* **1989**, *274*, 135–142.
- (14) Hayat, U.; Bartlett, P. N.; Dodd, G. H. *J. Electroanal. Chem.* **1987**, *220*, 287–294.
- (15) Yang, H.; Bard, A. J. *J. Electroanal. Chem.* **1992**, *339*, 423–449.
- (16) Vettorazi, N.; Silber, J. J.; Sereno, L. *J. Electroanal. Chem.* **1981**, *125*, 459–475.
- (17) Ekinci, D.; Tümer, F.; Demir, Ü. *J. Electroanal. Chem.* **2004**, *562*, 167–172.
- (18) Tokoyama, M. *Int. J. Mass Spectrom. Ion Processes* **1996**, *152*, 1–7.
- (19) Shacklette, L. W.; Wolf, J. F.; Gould, S.; Baughman, R. H. *J. Chem. Phys.* **1988**, *88*, 3955–3961.
- (20) Lien-Vien, D.; Colthup, N. B.; Fataley, B.; Grasselli, J. G. *The Handbook of Infrared and Raman Characteristic Frequencies of Organic Molecules*; Academic Press: New York, 1991.
- (21) Quillard, S.; Bayer, M. I.; Cochet, M.; Buisson, J. P.; Lovern, G.; Lefrant, S. *Synth. Met.* **1999**, *101*, 768–771.
- (22) MacDiarmid, A. G.; Zhou, Y.; Feng, J. *Synth. Met.* **1999**, *100*, 131–140.
- (23) Barclay, T. M.; Cordes, A. W.; MacKinnon, C. D.; Oakley, R. T.; Reed, R. W. *Chem. Mater.* **1997**, *9*, 981–990.
- (24) Zhang, Q. T.; Tour, J. M. *J. Am. Chem. Soc.* **1998**, *120*, 5355–5362.
- (25) Meng, H.; Wudl, F. *Macromolecules* **2001**, *34*, 1810–1816.
- (26) Bredas, L. *J. Chem. Phys.* **1985**, *82*, 3808–3811.

MA0499019